

REGION OF INTEREST DETECTION IN
THERMAL IMAGES OF DC MOTOR AND
AVERAGE TEMPERATURE CALCULATION

TUAN NUR ATIKAH BINTI TUAN SHUKRI

B.ENG (HONS.) ELECTRICAL
ENGINEERING (ELECTRONICS)

UNIVERSITI MALAYSIA PAHANG

UNIVERSITI MALAYSIA PAHANG

DECLARATION OF THESIS AND COPYRIGHT

Author's Full Name : TUAN NUR ATIKAH BINTI TUAN SHUKRI

Date of Birth : 17/11/1997

Title : REGION OF INTEREST DETECTION IN THERMAL IMAGES
OF DC MOTOR AND AVERAGE TEMPERATURE
CALCULATION

Academic Session : SESSION 2021/2022 - II

I declare that this thesis is classified as:

- CONFIDENTIAL (Contains confidential information under the Official Secret Act 1997)*
- RESTRICTED (Contains restricted information as specified by the organization where research was done)*
- OPEN ACCESS I agree that my thesis to be published as online open access (Full Text)

I acknowledge that Universiti Malaysia Pahang reserves the following rights:

1. The Thesis is the Property of Universiti Malaysia Pahang
2. The Library of Universiti Malaysia Pahang has the right to make copies of the thesis for the purpose of research only.
3. The Library has the right to make copies of the thesis for academic exchange.

Certified by:



(Student's Signature)



(Supervisor's Signature)

971117-29-5052
New IC/Passport Number
Date: 18/6/2022

Ahmad Afif bin Mohd Faudzi
Name of Supervisor
Date: 27 June 2022

NOTE: * If the thesis is CONFIDENTIAL or RESTRICTED, please attach a thesis declaration letter.

THESIS DECLARATION LETTER (OPTIONAL)

Librarian,
Perpustakaan Universiti Malaysia Pahang,
Universiti Malaysia Pahang,
Lebuhraya Tun Razak,
26300, Gambang, Kuantan.

Dear Sir,

CLASSIFICATION OF THESIS AS RESTRICTED

Please be informed that the following thesis is classified as RESTRICTED for a period of three (3) years from the date of this letter. The reasons for this classification are as listed below.

Author's Name
Thesis Title

Reasons	(i)
	(ii)
	(iii)

Thank you.

Yours faithfully,

(Supervisor's Signature)

Date:

Stamp:

Note: This letter should be written by the supervisor, addressed to the Librarian, *Perpustakaan Universiti Malaysia Pahang* with its copy attached to the thesis.



SUPERVISOR'S DECLARATION

I hereby declare that I have checked this thesis and in my opinion, this thesis is adequate in terms of scope and quality for the award of the degree of Electrical Engineering (Electronics).

A handwritten signature in black ink, appearing to read 'Ahmad', is written over a horizontal line.

(Supervisor's Signature)

Full Name : Dr. Ahmad Afif. Bin Mohd Faudzi

Position : Senior lecturer

Date : 27 June 2022

(Co-supervisor's Signature)

Full Name :

Position :

Date :



STUDENT'S DECLARATION

I hereby declare that the work in this thesis is based on my original work except for quotations and citations which have been duly acknowledged. I also declare that it has not been previously or concurrently submitted for any other degree at Universiti Malaysia Pahang or any other institutions.

A handwritten signature in black ink, appearing to read 'Atikah', is written above a horizontal line.

(Student's Signature)

Full Name : TUAN NUR ATIKAH BINTI TUAN SHUKRI

ID Number : EA18050

Date : 18/06/2022

REGION OF INTEREST DETECTION IN THERMAL IMAGES OF DC MOTOR
AND AVERAGE TEMPERATURE CALCULATION

TUAN NUR ATIKAH BINTI TUAN SHUKRI

Thesis submitted in fulfillment of the requirements
for the award of the
B.Eng (Hons.) Electrical Engineering (Electronics)

College of Engineering
UNIVERSITI MALAYSIA PAHANG

JUNE 2022

ACKNOWLEDGEMENTS

Praise to Allah the Almighty for His blessing and guidance. First and foremost, I want to express my heartfelt appreciation to Dr. Ahmad Afif bin Mohd Faudzi, my beloved supervisor, for providing invaluable assistance and regular suggestions during this project. Working and studying under his direction was a tremendous honour and privilege. From the first day I met him, I appreciated his unwavering support. The route to complete the Final Year Project will be more difficult without his help.

My family, especially my parents, deserve thanks for their love, support, prayers, and sacrifices throughout my life. I owe my parents a debt of gratitude for their patience and constant care for me. Thank you for assisting me in surviving all the stress and for not allowing me to give up. Also, thank you to my siblings for constantly brightening and delighting my days.

My profound gratitude also goes to my friends especially Muhammad Saiful Amin Bin Mohd Suhaimi for assisting me in finishing the thesis when I became overwhelmed and confused, as well as for their unwavering support in finishing the project. Also, to mention my friends from the Electrical and Electronic Engineering Department and other departments as UMP in assisting me in several ways throughout my research.

Last but not least, I would like to express my gratitude to everyone who was directly or indirectly involved in the completion of my Final Year Project. Thank you very much.

ABSTRAK

Haba adalah tanda awal kerosakkan atau kerosakkan peralatan yang biasa, oleh itu program penyelenggaraan pencegahan mesti dipantau dengan teliti. Pengiraan diperlukan dalam pemodelan haba motor untuk menghasilkan pekali haba perolakan. Pekali bergantung kepada suhu purata permukaan motor, yang boleh ditentukan dengan termokopel. Pilihan lain ialah menggunakan kamera pengimejan haba. Pengimejan terma berguna untuk mengesan kekurangan peralatan keseragaman dengan mengesan kawasan panas dan sejuk dalam suhu permukaan melalui tangkapan imej inframerah. Perisian Testo mempunyai alat had untuk menentukan kawasan ini, seperti segi empat tepat, segi empat sama, bulatan, dan elips kerana bacaan latar belakang yang mempengaruhi suhu purata ROI. Kertas ini bertujuan untuk mengesan Wilayah Kepentingan (ROI) dan untuk mengira suhu purata menggunakan kaedah ambang dan terakhir untuk membandingkan hasil antara Perisian Testo dan kaedah segmentasi.

ABSTRACT

Heat is a common early sign of equipment breakdown or malfunction, thus preventative maintenance programmes must be closely monitored. Calculations are required in motor thermal modeling to produce the convection thermal coefficient. The coefficient is dependent on the average temperature of the motor surface, which can be determined with a thermocouple. Another option is to use a thermal imaging camera. Thermal imaging is useful for detecting a lack of appliances uniformity by detecting hot and cold areas in surface temperature via infrared image capture. Testo Software have limitation tools to define these regions, such as rectangles, squares, circles, and ellipses because the background reading affecting the average temperature of ROI. This paper aims to detect Region of Interest (ROI) and to calculate average temperature that contains a segmentation algorithm by using Thresholding method and lastly to compare the result between Testo Software and Thresholding method.

TABLE OF CONTENT

DECLARATION	
TITLE PAGE	
ACKNOWLEDGEMENTS	ii
ABSTRAK	iii
ABSTRACT	iv
TABLE OF CONTENT	v
LIST OF TABLES	vii
LIST OF FIGURES	viii
LIST OF SYMBOLS	x
LIST OF ABBREVIATIONS	xi
CHAPTER 1 INTRODUCTION	1
1.1 Project Background	1
1.2 Problem Statements	2
1.3 Objectives	2
1.4 Scopes of Project	3
CHAPTER 2 LITERATURE REVIEW	4
2.1 Introduction	4
2.2 Flow of literature review	4
2.2.1 Image Pre-processing	4
2.2.2 Image Segmentation Algorithm	4
2.3 Thermal image	15

2.4	Motor	16
2.5	Region of Interest (ROI)	17
CHAPTER 3 METHODOLOGY		20
3.1	Introduction	20
3.2	Software and Function	20
	3.2.1 Python	20
3.3	Flowchart	21
	3.3.1 Flow of Programme	21
3.4	Data Acquisition	23
3.5	Calculation	23
CHAPTER 4 RESULTS AND DISCUSSION		25
4.1	Introduction	25
4.2	Results and Discussion	25
4.3	Analysis	30
CHAPTER 5 CONCLUSION		31
5.1	Conclusion	31
5.2	Future Recommendation	31
REFERENCES		32
APPENDIX A		35

LIST OF TABLES

Table 4-1 Comparing the result between Testo and Thresholding Method	30
--	----

LIST OF FIGURES

Figure 2-1 Prewitt edge detection filters	9
Figure 2-2 Horizontal and Vertical Sobel Edge	9
Figure 2-3 LoG Kernel	10
Figure 2-4 Robert Kernel	11
Figure 2-5 Examples of Regional Growth	12
Figure 2-6 Clustering	13
Figure 2-7 Condition monitoring applications of infrared thermography	15
Figure 2-8 Temperature steady-state against the type of components under different loads.	17
Figure 2-9 Testo's Software Shapes	18
Figure 2-10 Regular shapes are shown of a specific Region of Interest	18
Figure 2-11 Regions of Interest with the inclusion of irrelevant data or exclusion of data source	18
Figure 2-12 Original Image	19
Figure 2-13 Mask Image	19
Figure 2-14 Image after optimization	19
Figure 3-1 Process of programme	21
Figure 3-2 Original Image	22
Figure 3-3 Image converted into greyscale and image blurred was applied	23
Figure 3-4 Plot histogram for greyscale vs pixels	23
Figure 3-5 Binary threshold for masking	23
Figure 4-1 Comparison between Testo software and ROI which is testo have average temperature of 64.3°C meanwhile ROI 63°C	26
Figure 4-2 Comparison between Testo software and ROI which is testo have average temperature of 41.5 °C meanwhile ROI 43 °C	26
Figure 4-3 Comparison between Testo Software and ROI which is Testo have average temperature of 47.6 °C meanwhile ROI 53 °C	26
Figure 4-4 Comparison between Testo Software and ROI which is Testo have average temperature of 38.3 °C meanwhile ROI 39 °C	27
Figure 4-5 Comparison between Testo Software and ROI which is Testo have average temperature of 54.4 °C meanwhile ROI 57 °C	27
Figure 4-6 Comparison between Testo Software and ROI which is Testo have average temperature of 55.2 °C meanwhile ROI 58 °C	27
Figure 4-7 Comparison between Testo Software and ROI which is Testo have average temperature of 48.1 °C meanwhile ROI 55 °C	28

Figure 4-8 Comparison between Testo Software and ROI which is Testo have average temperature of 48.9 °C meanwhile ROI 55 °C	28
Figure 4-9 Comparison between Testo Software and ROI which is Testo have average temperature of 31.1 °C meanwhile ROI 34 °C	28
Figure 4-10 Comparison between Testo Software and ROI which is Testo have average temperature of 56.6 °C meanwhile ROI 56 °C	29
Figure 4-11 Comparison between Testo Software and ROI which is Testo have average temperature of 64.1 °C meanwhile ROI 64 °C	29

LIST OF SYMBOLS

μ	Micro
δ	Delta

LIST OF ABBREVIATIONS

ROI	Region of Interest
TH	Thermographic
VIS	Visual

CHAPTER 1

INTRODUCTION

1.1 Project Background

In motor thermal modelling, calculations are needed to produce the convection thermal coefficient. The coefficient requires average temperature on the motor surface, which can be measured using a thermocouple. Another way is using thermal image camera.

Thermal imaging is based on infrared energy (known as heat which is emitted from all objects. This infrared emitted by an object is known as its heat signature. In general, the hotter an object is, the more radiation it emits [1]. Thermal imaging technology is widely employed in a variety of industries. Thermal imaging cameras were first created for military usage during the Korean War and since then have migrated into a variety of fields and applications. For example, electrical maintenance, plumbers, mechanical and building construction technicians, animal and pest management, transport navigation, healthcare and medicine, fire-fighters, police, science, and research [1][2][3][4]. Thermal image cameras have developed into tiny systems it seems like a conventional video camera, are easy to operate, and provide a real-time high-resolution image by detecting abnormalities that are typically invisible to the naked eye. Thermal image segmentation is useful in various applications. The thermal image contains much information regarding the motor and this information could be obtained using various image processing techniques. In addition, the simplest technique to locate the thermal image hotspot is by applying image segmentation method [5]. From the segmentation results, it is possible to identify the region of interest (ROI) and object in the scene, which is very beneficial to the subsequent image analysis. There are many techniques of segmentation that will be discussed in Chapter 2.

Motor is used in various industries. As the technology that goes into motors has become more complicated, technicians and engineers need to know what causes electric motor failure. The difficulty is that the reasons for electric motor failure are nuanced and complex because a variety of factors might contribute to a problem that eventually leads to a motor failure [6]. Worn-out bearing and defective winding insulation are two of the most common causes of industrial motor failure [5]. However, these problems could be caused by several circumstances, including power quality issues, mechanical issues, installation issues and variable frequency drive issues.

The testo IRSOFT software is used for the analysis, processing and archiving of the images recorded by a testo thermal image. It also has integrated reporting for the clear presentation of the data. The settings can be performed on the connected thermal image via the instrument control. However, the software has their own limitation especially in manual cropping. This paper is to reduce the shortcoming of this software.

1.2 Problem Statements

Testo software is used to analyse the thermal image in detail, but there is certain problem regarding this software. One of the problems is, selection of area is limited because it is depending on geometry that already given such as oval, circle, and rectangular. Not only that, in order to set the ROI, the user need to manually define the desired area. It is not ideal for professional use, and this step can take time as stated that the region of interest needs to be defined manually. This kind of limitation will make the software inconvenient for the user.

Due to the limitation of the ROI geometry, this also leads to inaccurate reading of thermal image, because background reading also affected the output value. The reason behind this is with the given ROI tools, most of the time the shape of ROI is not properly aligned to the desired area, thus leading to background reading also in the ROI's area.

1.3 Objectives

- 1) To detect the Region of Interest (ROI).

- 2) To calculate the average temperature that contain segmentation algorithm by using thresholding method.
- 3) To compare the result between Testo Software and thresholding method.

1.4 Scopes of Project

- 1) 22 samples data was used.
- 2) The image was taken by using Testo 865 thermal imaging camera.
- 3) The resolution of the image is 160x120 pixels.

CHAPTER 2

LITERATURE REVIEW

2.1 Introduction

This chapter briefly discusses the literature review and conclusions from earlier studies that other researchers conducted to use image segmentation methods in many domains, including maintenance area, using various models for identification, classification, and detection. A good literature review not only compiles sources, but also analyses, synthesizes, and critically evaluates to provide a complete picture of the current state of knowledge on the subject. There are numerous techniques for increasing and determining greater accuracy.

2.2 Flow of literature review

2.2.1 Image Pre-processing

Image pre-processing is the steps taken to format an image before it is used by modelling and inference training. Eliminating low-frequency background noise, levelling the intensity of individual particle images, removing reflections, and masking sections of images are all part of the data image enhancement process [7].

2.2.2 Image Segmentation Algorithm

Image segmentation is a technique in digital image processing that divides a digital image into subgroups called image segments, reducing the image's complexity and making subsequent processing or analysis easier. Segmentation, to put it another way, is the process of assigning labels to pixels. All picture elements or pixels that belong to the same category are given the same label. Image objects are the parts into which the image is divided. The popular techniques used for image segmentation are thresholding, edge

detection, region-based, clustering, watershed, and artificial neural network-based techniques which are describe as follows.

2.2.2.1 Thresholding

One of the most important approaches in image segmentation is the threshold technique. When analyzing the thermal health of electrical equipment, the thresholding approach is a very useful tool for distinguishing the warm area from its background. This algorithm gives a binary output from a greyscale image. Pixels with a bit value of zero are converted to black, while pixels with a bit value of one are converted to white (a bit value of one). In some cases, thresholding is described as separating foreground (black) and background (white) values in an image (white). There are two sorts of thresholds: single level and multilevel. By applying a threshold value to the image, possible thermal anomalies in the equipment can be discovered [8]. If the original image is $I(x, y)$, the threshold image, $G(x, y)$ is defined as

$$G(x, y) = \begin{cases} 1, & \text{if } I(x, y) > T \\ 0, & \text{if } I(x, y) \leq T \end{cases} \quad 2.1$$

Where T is the threshold value. The segmentation result is represented as a binary image, with 1 indicating the target object or region and 0 representing the background image. Single level thresholding is the name for this method of thresholding. A slightly more general use of this principle is multilevel thresholding, in which the image histogram is defined by three dominant modes (for example, two types of light objects on a dark background). Multilevel thresholding classifies point (x, y) as belonging to one object class if $T1 < f(x, y) \leq T2$, to the other object class if $f(x, y) > T2$ and to the background if $f(x, y) \leq T1$: where $T1$ and $T2$ are the two thresholds selected for the image [9].

i. Global

In Global threshold, T is used as a single value denoting the threshold for all picture pixels. This thresholding approach is known as global thresholding because T is entirely dependent on $f(x, y)$ (in other words, only on gray-level values) and the value of T is solely related to the character of pixels. Minimum thresholding, Otsu, optimal

thresholding, histogram concave analysis, iterative thresholding, entropy-based thresholding, and so on are examples of global thresholding approaches [10].

The most basic thresholding strategy uses a single global threshold, T , to segment the image histogram. The image is then divided pixel by pixel, with each pixel labelled as an object or background depending on whether the grey level of the pixel is greater or less than the value of T [9].

Apart from that, Binary Thresholding is the most used thresholding technique. The same threshold value is used for each pixel. If the pixel value is less than or equal to the threshold, it is set to 0, otherwise it is set to the maximum value. A very simple approach of segmentation contains associating a binary number with each pixel of the image f that is dependent on the intensity of the pixels and a threshold “ T ”.

$$G(x, y) = \begin{cases} 1, & \text{if } f(x, y) \geq T \\ 0, & \text{if } f(x, y) < T \end{cases} \quad 2.2$$

a) Otsu’s Method

Otsu’s method is a means of automatically finding an optimal threshold based on the observed distribution of pixel values. For thermal image processing [5] this method has been frequently used to detect the warmest locations. The Otsu's threshold is determined by searching the entire range of the image's pixel values until the intra-class variances are at their lowest. The threshold calculated by Otsu's technique is more fundamentally determined by the class with the largest variance, whether it is the background or the foreground, as defined. As a result, when the image's histogram contains more than two peaks or one of the classes has a big variation, Otsu's approach may produce suboptimal results [11].

However, the original image segmentation methods will undoubtedly cause faults in image processing, and these flaws will affect the image processing and recognition outcomes. [12] use Otsu’s method and genetic algorithms for image segmentation, a genetic algorithm can effectively identify the global optimal parameter value space.

b) Iterative

In this technique, approximate threshold is successively refined to get a new value to partition the image better where μ_1, μ_2 are means [13].

$$T = \frac{1}{2}(\mu_1 + \mu_2) \quad 2.3$$

At iteration n , as a new threshold T_n is established using the average for the foreground and background class means [14].

c) Entropy-Based

Entropic thresholding methods exploit distribution of the grey levels in the scene [15]. The information between the foreground and background distributions in the image is maximized by increasing the entropy of the thresholded image.

d) Histogram

Histograms are a visual representation of data counts grouped into predefined bins. The number of pixels in each bin's range is counted, and the resulting image is produced. Axis x indicates the bins, whereas axis y indicates the number of pixels in each bin. One of the most used techniques for monochrome image segmentation is histogram thresholding. It is assumed that the images are made up of region with various grey levels [16]. The range of a data set is divided into equal-sized classes to create histograms. The number of points in each class from the data set is then counted for each class.

This class of techniques achieves thresholding while maintaining the histogram's structure qualities. Basically, two most significant pinnacles and an interceding valley is scanned for utilizing such apparatuses because the protrusive structure of the histogram, or its ebb and flow and 0 (zero) intersections of the wavelet components [17]. Elective creators use two-advance capacity or two-shaft autoregressive smoothing to estimate the histogram.

ii. Local

When background elimination is uneven, global thresholding strategies can fail. In such cases, it is usual practice to pre-process the image to compensate for the elimination problems before applying a global threshold to the pre-processed image.

Thresholding $f(x, y)$ with a locally variable threshold function $T(x, y)$ is equivalent to this [9]:

$$g(x, y) = \begin{cases} 1, & \text{if } f(x, y) \geq T(x, y) \\ 0, & \text{if } f(x, y) < T(x, y) \end{cases} \quad 2.4$$

Local thresholding occurs when the threshold T is dependent on both $f(x, y)$ and $p(x, y)$. This approach separates an original image into subregions and selects appropriate thresholds T_s for each subregion. Gray level filtering must be used after thresholding to remove discontinuous grey levels between sub images. Simple statistical thresholding, 2-D entropy-based thresholding, histogram-transformation thresholding, and other local thresholding approaches are common [10].

By cropping the original image into 16 equal portions, local thresholding [16] is performed. After cropping, OTSU's algorithm is applied to each cropped part separately, resulting in a separate threshold for each cropped portion. As a result of this, the original image is segmented using a locally created threshold.

iii. Adaptive

A perfect segment histogram can be converted to a histogram that cannot be efficiently separated by a single global threshold due to imaging issues such as uneven removal. Split the original image into sub-images and then divide each sub-image using a separate 't' threshold to avoid this issue. Because the threshold applied to each pixel is defined by its location in terms of sub-images, this form of threshold is adaptive [9].

2.2.2.2 Edge Detection

Edge detection is an image processing technique for detecting points in a digital image where there are discontinuities or abrupt changes in image brightness. The image's borders (or boundaries) are the points where the brightness of the image varies dramatically. There are a variety of approaches, and the following below shows are some of the methods commonly used.

1. Canny

The Canny technique is an useful way to locate edges in images by isolating noise from the image before finding edges without impacting edge features, and then using the tendency to find edges and critical threshold values. The edge detection algorithm identifies edges with minimal error and edge points that are precisely localized, as well as edges that have been marked only once in an image [18].

2. Prewitt

The Prewitt Edge filter uses horizontal and vertical filters to detect edges. The two filters are applied to the image and then combined to get the result. These carriers can be separated and are less expensive than Sobel. Prewitt operators' biggest challenge is their sensitivity to noise [18]). Prewitt edge detector uses the following mask to approximate digitally the first derivatives G_x and G_y [19].

-1	0	1
-1	0	1
-1	0	1

G_x

1	1	1
0	0	0
-1	-1	-1

G_y

Figure 2-1 Prewitt edge detection filters

3. Sobel

In a grayscale image, the Sobel operator determines the gradient magnitude and direction at each pixel. An edge is formed by pixels with a large magnitude. Since Sobel is the same as Prewitt, there is only one difference which are Sobel operator has '2' and '-2' values in center of first, third column of horizontal mask and first, third rows of vertical mas [20].

-1	-2	-1
0	0	0
1	2	1

-1	0	1
-2	0	2
-1	0	1

Figure 2-2 Horizontal and Vertical Sobel Edge

4. Laplacian of Gaussian (LoG)

The Laplacian is a 2-D isotropic measure of an image's second spatial derivative. After filtering $f(x, y)$ with a Laplacian of Gaussian filter, this detector examines for zero crossings to locate edges. The Laplacian is frequently used to minimize the sensitivity of an image that has been smoothed with something like a Gaussian Smoothing filter [21]. To solve this problem, the noise should first be minimized by using a Gaussian smooth filter. After that, a Laplacian filter must be applied to the image. Equation below shows how to calculate the Laplacian pixel density value.

$$L(x, y) = \frac{\partial^2 I}{\partial x^2} + \frac{\partial^2}{\partial y^2} \quad 2.5$$

The LoG filter, which is particularly successful in image processing applications and has a lower noise level, is commonly used 3x3 kernels, as illustrated in Figure 2-3 below [22].

1	1	1	-1	2	-1
1	-8	1	2	-4	2
1	1	1	-1	2	-1

Figure 2-3 LoG Kernel

The Laplacian operator is used to improve the blurring effect due to the blurring effect, since it conforms to the descent model. In the imaging process, the diffusion effect occurs frequently [23].

5. Robert

The Robert edge detection operator has a fast and simple structure. The primary idea behind this operator is to use discrete differentiation to approximate the gradient of an image. It has 2x2 convolution kernels and as shown in Figure 2-4 these two convolution kernels are rotated 90° to each other.

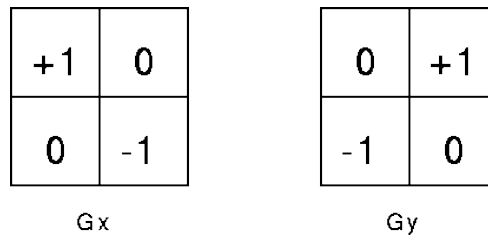


Figure 2-4 Robert Kernel

The Gx mask is simply rotated at 45° and Gy is obtained. These two masks can be applied to the image for detecting edges [24].

2.2.2.3 Region-Based

Images are divided into sections with similar properties using the region-based segmentation method. The way to find this group is to select a seed point, which can be a small part of a large part of the input image. A region-based segmentation algorithm would either increase or reduce the number of pixels in the seed points, allowing them to be combined with other seed points once they were located. Region-based segmentation can be divided into two categories based on these two methods below.

1. Region Growing

Pixels representing homogeneous regions in the image were grouped using a region growth algorithm. Areas are formed by collecting neighbouring pixels of different qualities with less than a certain amount, such as intensity. Each expanded area is assigned its numerical label in the output image. When borders are difficult to discern in noisy photos, region-growing algorithms perform better. Homogeneity is an important attribute of regions, and it is employed as the primary segmentation criterion in region growth, which divides a picture into zones with the most homogeneity [9].

Figure 2-5 below shows is an example of a known seed location for region growing. The necessity to separate the image is seen in Figure 2-5 (a). Two seed pixels (indicated as grey squares) are known to be prepared for regional growth. The pixel is included in the region where the seed pixel is located if the absolute value of the grey value difference between the pixel and the seed pixel is regarded to be smaller than a specific threshold T . The regional growth findings at $T = 3$ are shown in Figure 2-5 (b), and the figure is well separated into two sections. The findings of region growth at $T = 6$ are shown in Figure 2-5 (c), and the entire plot is in an area [23].

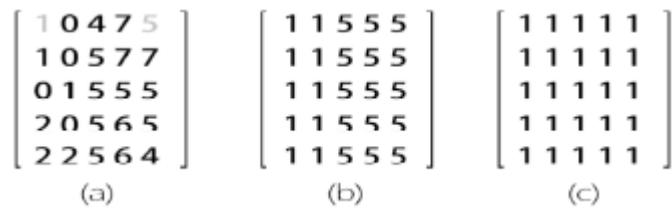


Figure 2-5 Examples of Regional Growth

Regional growth [23] has the advantage of separating connected regions with similar features and providing accurate boundary information and segmentation results. Regional growth is a basic concept that only requires a few seed locations to implement. Furthermore, the expanding process's growth conditions can be freely specified. Finally, it can choose many criteria at once.

2. Region Splitting and Merging

The entire image is first taken as a single region in region splitting. If the region does not meet the specified rules, it is divided into numerous regions (typically four quadrants), and the predefined rules are applied to those regions to determine whether to further subdivide or classify the region. The method in region splitting considers the entire image, whereas in region growth, the algorithm focuses on a single location. The process is repeated until no further separation of regions is required, for example each region follows the predetermined regulations. Every pixel is treated as a separate zone in the region merging approach.

The algorithm for merging [9] represents a general approach to region merging segmentation. The definition of the beginning segmentation and the criterion for merging varied between approaches.

The most basic approach starts by grouping the image into an area of 2 x 2, 4 x 4 or 8 x 8 pixels. The region description is compared with the description of another region, and if it matches, it is combined into a larger part, and a new region description is calculated. Mismatched areas were identified as unsuitable. All neighbouring regions, including newly emerged ones, are continuing to merge. When a region cannot be combined with any of its neighbours, it's labelled 'final,' and the merging process is complete after all image regions have been labelled this way.

Region splitting methods generally use similar criteria of homogeneity as region merging methods and differ only in the direction of their application.

2.2.2.4 Clustering

Clustering is the process of dividing a set of data into a certain number of clusters, each with similar features amongst the data points [23]. Clusters are made up of data points that have been clustered together to reduce the amount of space between them. A set of similar elements is referred to as a “class”. Clustering is done in accordance with standards and rules that control how items are classified throughout the process. The feature space is segmented based on their aggregate in the feature space, and then the segmentation result is transferred back to the original picture space.

Several studies have been carried out in the subject of image segmentation by clustering. There are several approaches, with the K-Means clustering algorithm being one of the most widely used.

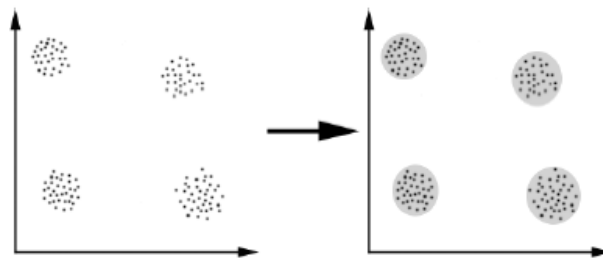


Figure 2-6 Clustering

One of the most frequently used methods is K-Means clustering. Based on the distance metric used for clustering, it divides the data points into k clusters. The user is responsible for determining the value of 'k.' The distance between the data points and the cluster centroids is determined [23].

The index of similarity or dissimilarity between pairs of data components is used in the K-mean technique [25]. The K-means algorithm is a method that is iterative, numerical, non-numerical, and unsupervised. This sort of technique is popular because of its ease of use and implementation. It is frequently used to group pixels in an image. The use of spatial and shape information in clustering methods is becoming more common.

2.2.2.5 Watershed-Based

In image processing, a watershed is a grayscale picture change. It refers to a geological watershed or a drainage boundary. A watershed method would be used to treat the image as if it were a topographic map. It looks for the lines that run along the tops of the ridges using the brightness of a pixel as its height.

Watershed is a technical term with a wide range of definitions and applications. Apart from recognising the pixels' ridges, it focuses on defining basins (the opposite of ridges) and flooding the basins with markers till they reach the watershed lines of the ridges. Because basins have more markers than ridges, the image is separated into multiple portions based on each pixel's 'height.'

The watershed approach is used to transform each image into a topographical map. The grey values of their pixels would reflect the topography of the watershed segmentation approach. On the other hand, a landscape with slopes and hills would surely have three-dimensional elements. As a result of the image's three-dimensional representation, the watershed would create places known as "catchment basins."

2.2.2.6 ANN

A neural network is a computer model of the human brain that attempts to mimic its learning process. In recent years, artificial neural networks (ANNs) have been widely used to solve the problem of medical image segmentation. Many parallel nodes make up a neural network based on life modelling, particularly the learning process of the human brain [25]. Each node can do some fundamental computations. Transferring connections between nodes and connection weights can help with the learning process. Although Neural Nets are time-consuming when training the data, the results have been encouraging, and the application of these has been highly successful. Many age segmentation approaches suffer from this issue. Two key steps are included in the neural network segmentation method which are using a neural network, extracting features, and segmenting images [25].

2.3 Thermal image

Abnormal behaviour temperature distribution can be caused by faulty machinery, corroded electrical connections, broken material components, and so on. The infrared region of the electromagnetic spectrum is emitted by every object having a temperature greater than 0 K (*i. e.*, $273\text{ }^\circ\text{C}$). Infrared radiation (*wavelengths of 0.75– 1000 lm*) is found in the electromagnetic spectrum between microwaves and visible light [4]. One of the core parts of this project is using thermal image to diagnose electric motor. Motor control centres, transformers, substations, and switchgears, capacitor banks, overhead power lines, drives, light and power panels, power cables and trays, terminal strips, and power supplies are all examples of electrical equipment that can be monitored using IRT [4]. In [26] present a method for biometric recognition based on hand images obtained by a thermographic camera that contains a visible (VIS) and a thermographic (TH) sensor. Due to imbalance load, [26] has obtained a new hand image database with a thermal camera, TESTO 882-3, that offers both a visual and a thermal image of local hot regions. This paper also discussed a vital technique for detecting electrical faults using thermal image segmentation [27].

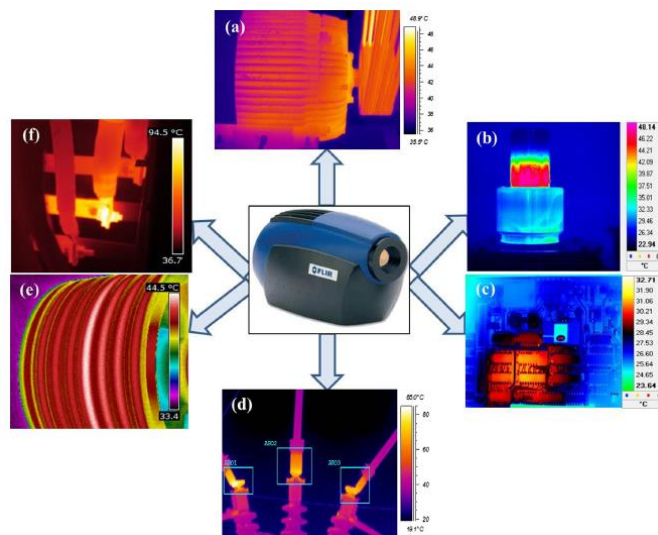


Figure 2-7 Condition monitoring applications of infrared thermography

The figure above is taken from [4] shows various condition monitoring applications of infrared thermography. (a) Monitoring of machinery where abnormal surface temperature distribution indicates a probable flaw. (b) Inspection of liquid levels in industrial components. (c) Review of printed circuit boards. Localized defects like short circuits or current leakages produce hot spots easily detected by infrared

thermography. (d) Typical thermal images of a transformer circuit breaker where the faulty regions can be seen as hot spots. (e) Inspection of shaft belt where the thermal anomaly is due to over-tightening of a belt. (f) Condition monitoring of three-phase electrical panels where local hot spots are developed due to load imbalance.

In [28] introduced a new image processing system for extracting the human forearms region from infrared thermal images automatically. By segmenting the contours of an object in thermal images and analysing the data from each foreground fragment, the heat signature of an object was identified. Due to the limitations of thermal sensors, manually contouring thermal images is difficult and time intensive (e.g., a high signal-to-noise ratio and low contrast). In [29] propose a semiautomatic segmentation method that incorporates data from a second optical camera. In [30] present a comparison of different ROIs using image segmentation algorithm. The implementation of a segmentation method helps in the improvement of thermal image analysis accuracy.

2.4 Motor

Motor failure as its application in rotating electrical machinery, such as electric motors, may not be as straightforward. Referring to Figure 2-8 below, the figure shows the temperature of a small dc motor's component during operation with the various load. The figure was taken from [31]. There are 4 main features monitored: brush, bearing, casing and permanent magnet. The motor was tested under 3 conditions of load, which are represented by the current value. The lowest current, 0.7A, indicates a lower load, and the maximum current (3.5A) indicates a full load. Based on the figure, it can be concluded that each component gets hotter with more load. So, the temperature between 30 – 60 can be considered normal for a motor under a load.

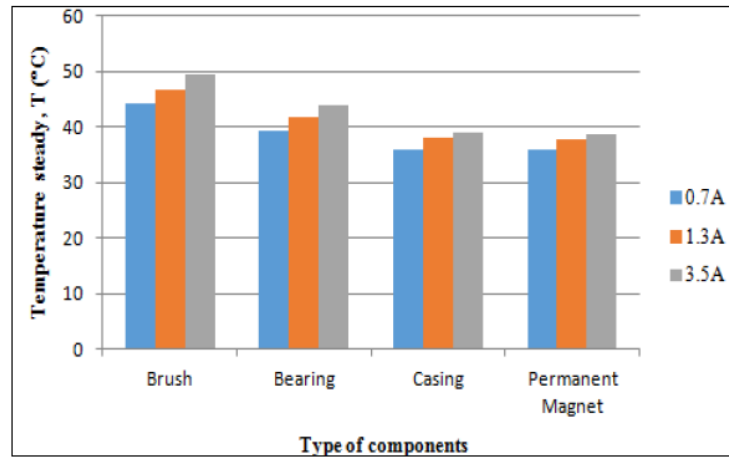


Figure 2-8 Temperature steady-state against the type of components under different loads.

2.5 Region of Interest (ROI)

The region of interest (ROI) in an image is defined by a binary mask. Image pixels with mask pixel values of 1 correspond to the ROI. Image pixels that have a mask pixel value of 0 are displayed as part of the foreground.

ROI can be made up of continuous or discontinuous clusters of pixels, depending on the purpose. A single set of related pixels is referred to as an adjacent region. A single object in a picture could be represented by a contiguous ROI, such as one car in a street scene or body tissue in a medical scan. A discontinuous ROI, for example, may represent all pixels in an aerial photograph that belong to water or all tumorous cells in a medical image.

In Testo's software uses regular shapes to define these regions, such as rectangles, squares, circles, and ellipses that poorly identify certain regions (see Figure 2-9). Figure 2-10 illustrates two typical geometric shapes to define a specific ROI. When these regular geometric patterns do not match the anatomical shape of the area to be defined, they impose limitations on the interpretation of thermal imaging, either by excluding pertinent data or including irrelevant data as Figure 2-11. This can lead to the inclusion of errors or misunderstandings in the analysis of a specific thermal image.

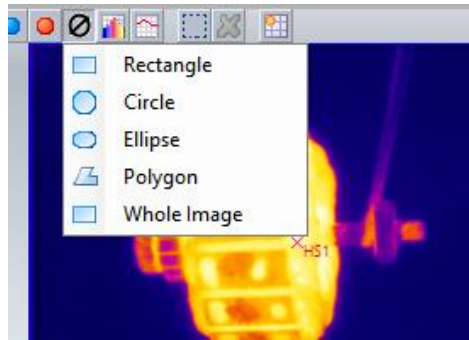


Figure 2-9 Testo's Software Shapes

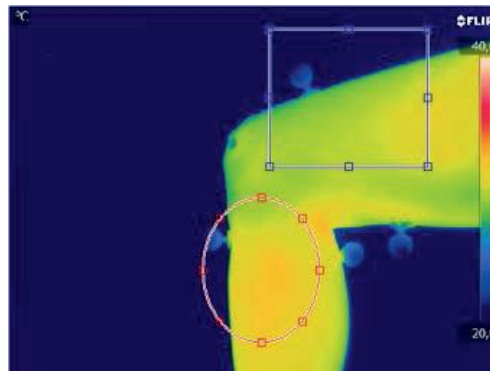


Figure 2-10 Regular shapes are shown of a specific Region of Interest

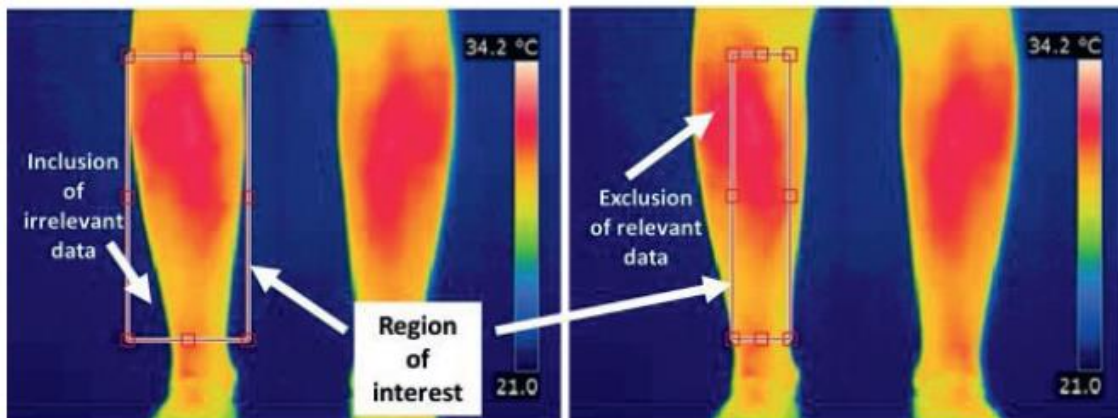


Figure 2-11 Regions of Interest with the inclusion of irrelevant data or exclusion of data source

The RGB image model (R for Red, G for Green and B for Blue) is considered the most appropriate for an image processing [30]. Setting some pixel values in an image to zero or another "background" value is known as masking. There are two methods for masking which are the pixel intensity of the resulting masked image will be set to the background value wherever the pixel intensity value in the mask image is zero (usually zero) and using a set of ROIs as the mask. The ROIs for each slice are used to define the mask. Figure 2-12 shows the original image, Figure 2-13 Mask Image and Figure 2-14 Image after optimization.

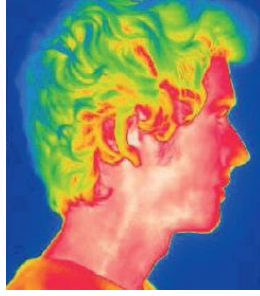


Figure 2-12 Original Image



Figure 2-13 Mask Image



Figure 2-14 Image after optimization

CHAPTER 3

METHODOLOGY

3.1 Introduction

This chapter is about the experimental procedure taken for this project this will include explaining the method used to detect the ROI, and python to later provide the desired output. As stated in chapter 1, the objective of this project is to use Thresholding method to calculate the average temperature and to compare the result between Testo Software and segmentation method. Then, the flow for this project will be explained in this chapter. The methodology for this project comprises thresholding methods and python to provide the output so that the objective is fully achieved.

3.2 Software and Function

3.2.1 Python

Python is one of the most widely used programming languages in both academia and industry for machine learning. When it comes to Machine Learning, NumPy provides a wealth of valuable support functions. NumPy is a widely used library for storing and computing with numerical arrays. Because most NumPy functions are implemented in C for performance, this not only allows for more concise code, but it also speeds up the code. Colab is a Google Cloud-based Python development environment that runs in the browser. Colab is a direct-access virtual machine.

3.3 Flowchart

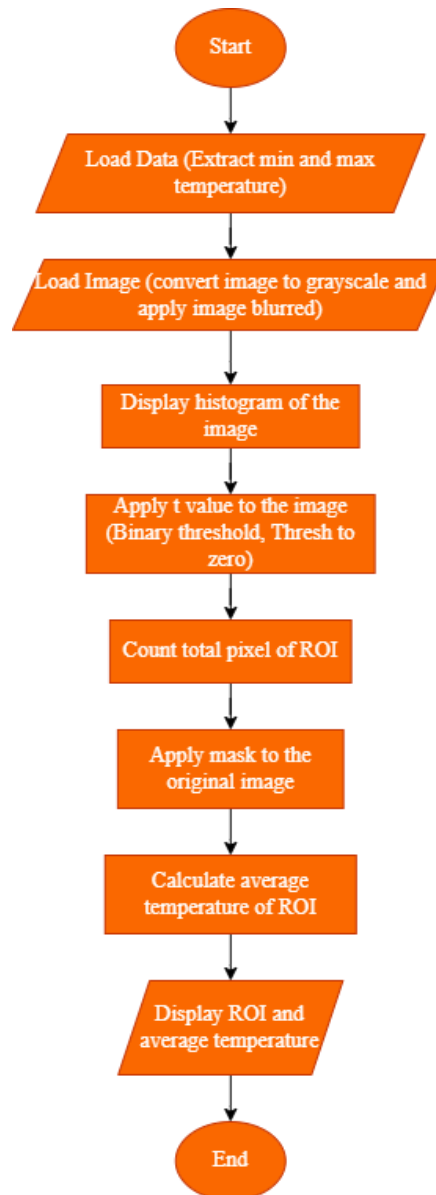


Figure 3-1 Process of programme

3.3.1 Flow of Programme

To get a general understanding of this project, provided above shows the flowchart for this project. At the very beginning of this flowchart, the user needs to upload the excel data to Google Colab that can execute arbitrary python code through the browser which contain the data which are minimum, maximum, and average temperature from Testo Software that taken from thermal imaging camera. Next, the user also needs to upload the thermal image to the programme. The image is converted into greyscale and apply image blurred. A greyscale image is mostly made up of two colours which is black

and white. It contains information about intensity, with the black representing the lowest intensity and white representing the highest intensity. Then, the next process is to display the histogram of the image. The histogram will show the visual info to fixed the value of T . After that, apply T value to the image by using binary threshold and thresh to zero. As mentioned in chapter 2 above, binary threshold is if the pixel intensity is greater than the set threshold, value set to 255, else set to 0 (black). Thresh to zero is to count the total intensity. The range of T will be black and the value in T range will be in greyscale format. Next, it will count the total pixels of ROI and apply masking to the original image. Then, the last process is to calculate average temperature of ROI. In the final step, it will display the ROI and average temperature of the DC motor. Figure below shows the process of the programme before getting the output.

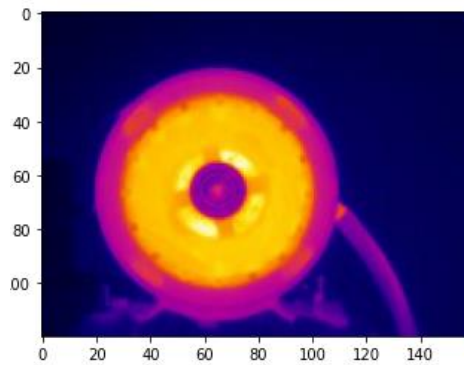


Figure 3-2 Original Image

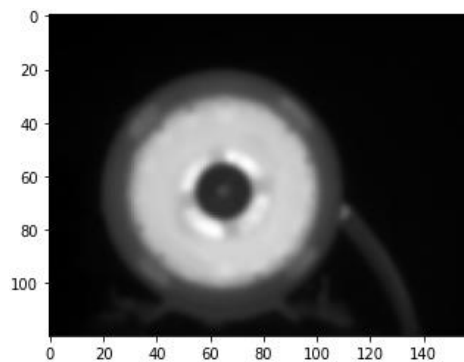


Figure 3-3 Image converted into greyscale and image blurred was applied

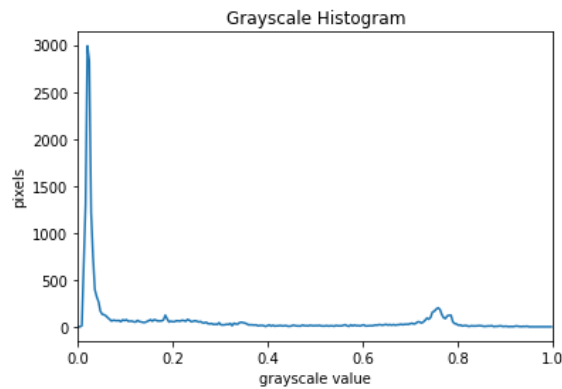


Figure 3-4 Plot histogram for greyscale vs pixels

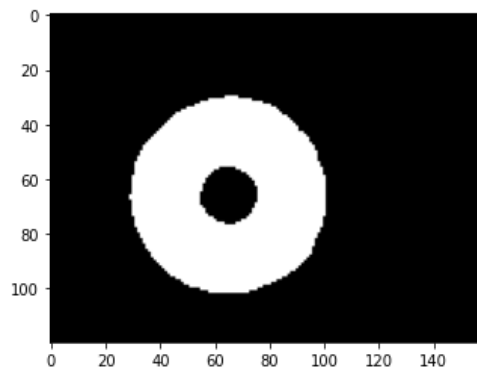


Figure 3-5 Binary threshold for masking

3.4 Data Acquisition

For the purpose of this work, by using Testo 865 Thermal Image Camera which provided a resolution of 160 x 120 pixels. There are 22 samples used as a reference and benchmark for this project, these sample consists of variety of motor's angles, loads, and types. The thermal image is processed using the provided Testo software.

3.5 Calculation

This project is based on image segmentation, thresholding method to be precise. Firstly, in order to achieve image segmentation, the author take all the sample images and manually find the threshold value for each sample. After that, all the threshold value will be used to find the average threshold value, which is 0.4.

There are three thresholds in this project, the first one is for masking, second one is used to count the pixels value and the last one is to find the sum value of an intensity.

The first threshold value is set between the range of 0 to 1, meanwhile the other two thresholds is between the range of 0 to 255. To make the second and third threshold, follow the first one the ratio of 1:255 is used to convert the range. So, every time the first threshold value is changed, the other two threshold will automatically follow the changes.

$$\begin{aligned}
 t &= 0.4 \text{ (average sample)} && 3.1 \\
 \text{Threshold range} &= 0 \text{ to } 255 \\
 \text{ratio} &= 1:255 \\
 t_int(\text{variable}) &= \frac{t}{0.0039215686274}
 \end{aligned}$$

For this project, it utilized the colour intensity of greyscale image, which is 0 to 255, 0 represent as black meanwhile 255 represent as white. In order to convert the intensity value into degree Celsius, data from Testo's excel will be loaded into the programme to extract the minimum and maximum value. The reason this value is needed because the author needs to set temperature range before converting the result into degree Celsius. Referring 3.2 to calculation below for the average temperature, the ratio of intensity and temperature can now be calculated.

$$\begin{aligned}
 \text{Range} &= \text{maximum} - \text{minimum (from data)} && 3.2 \\
 \text{ratio of temperature} &= \frac{\text{range}}{255} \\
 \frac{\text{total sum of intensity in ROI}}{\text{total pixels in ROI}} &= (\text{intensity unit}) \\
 \left(\left(\frac{\text{total sum of intensity in ROI}}{\text{total pixels in ROI}} \right) \right) \times \text{ratio of temperature} & \\
 + \text{minimum data of temperature} &
 \end{aligned}$$

CHAPTER 4

RESULTS AND DISCUSSION

4.1 Introduction

This chapter will be explaining the result from a programme of ROI and average temperature using Google Colab. From that, the output of ROI and average temperature will be observed.

4.2 Results and Discussion

To perform this research work, 22 samples of thermal image DC motor were analysed. Below are a couple of sample image used to make a comparison of ROI by using Testo and thresholding method.

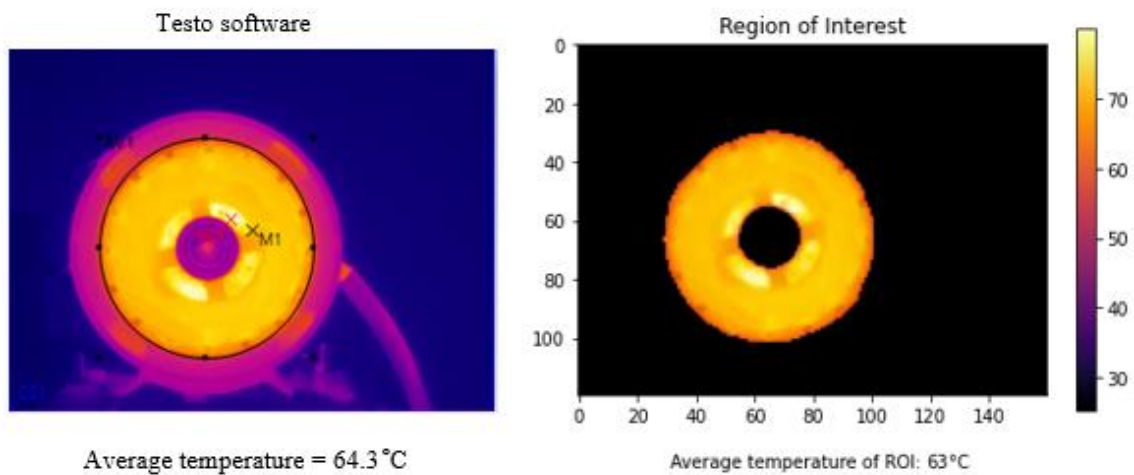


Figure 4-1 Comparison between Testo software and ROI which is testo have average temperature of 64.3°C meanwhile ROI 63°C

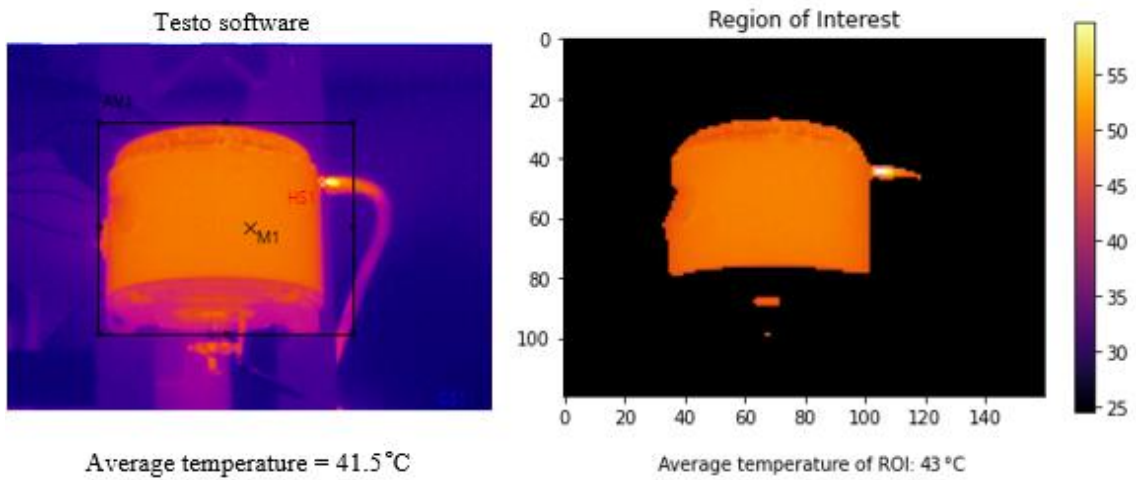


Figure 4-2 Comparison between Testo software and ROI which is testo have average temperature of 41.5 °C meanwhile ROI 43 °C

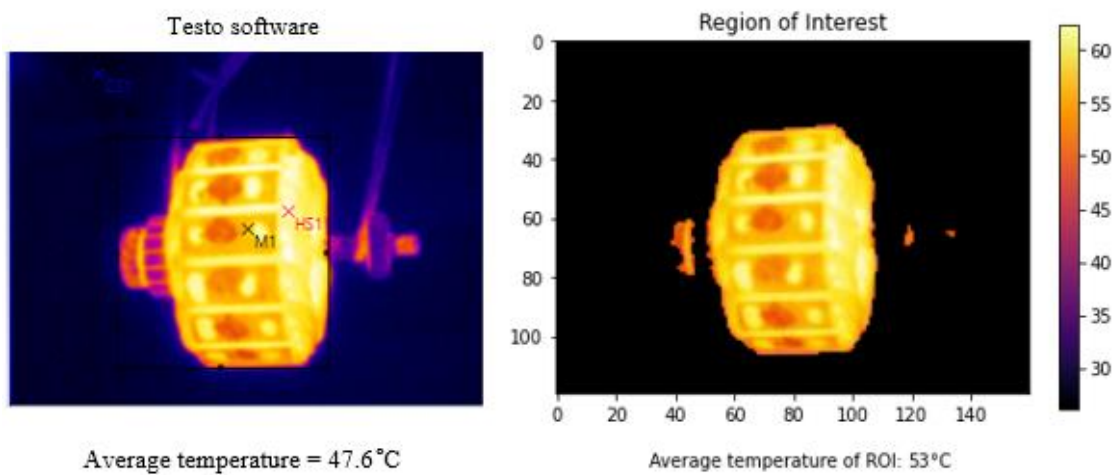


Figure 4-3 Comparison between Testo Software and ROI which is Testo have average temperature of 47.6 °C meanwhile ROI 53 °C

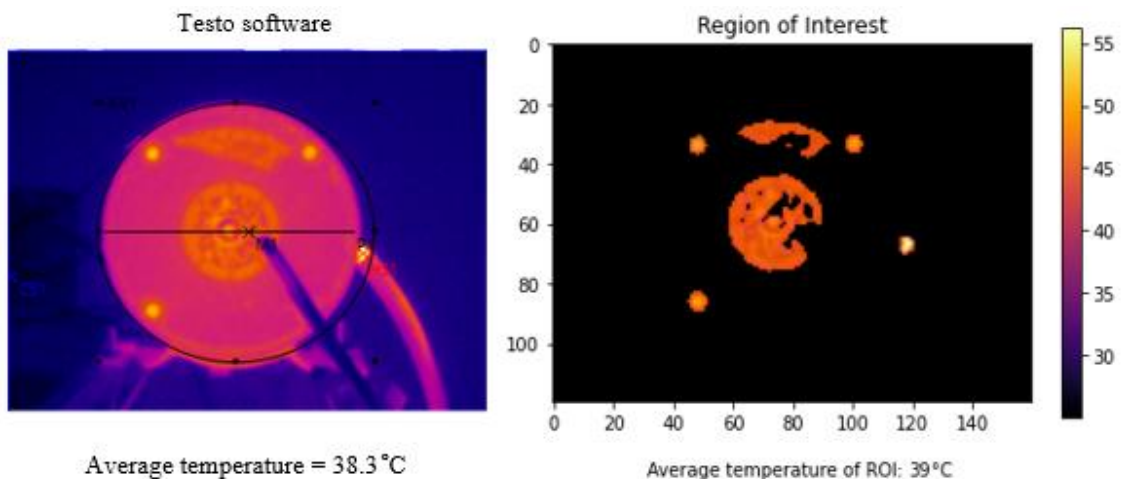


Figure 4-4 Comparison between Testo Software and ROI which is Testo have average temperature of 38.3 °C meanwhile ROI 39 °C

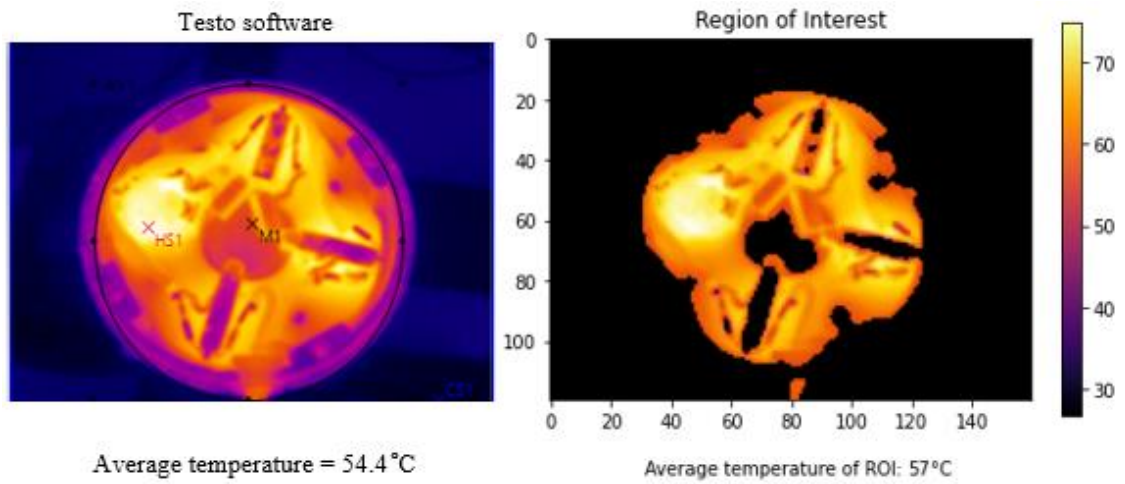


Figure 4-5 Comparison between Testo Software and ROI which is Testo have average temperature of 54.4 °C meanwhile ROI 57 °C

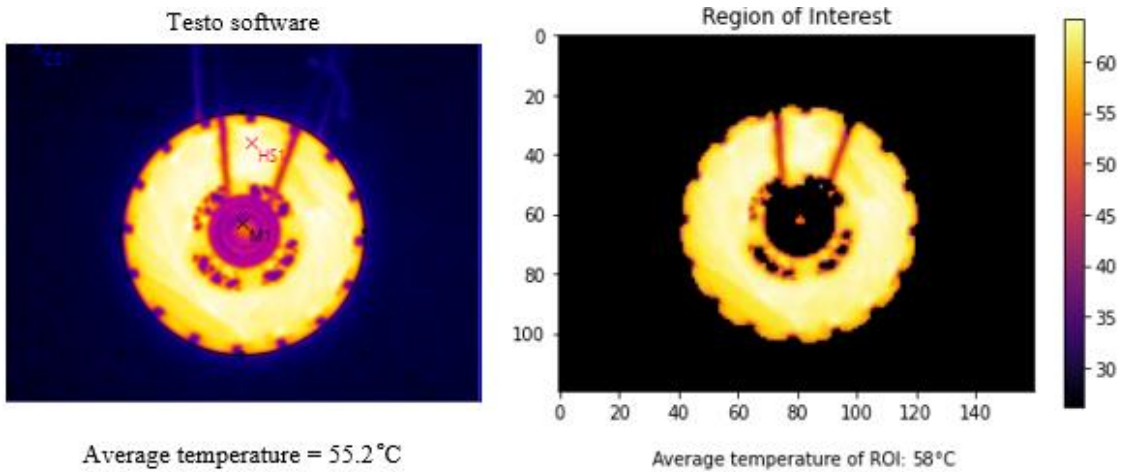


Figure 4-6 Comparison between Testo Software and ROI which is Testo have average temperature of 55.2 °C meanwhile ROI 58 °C

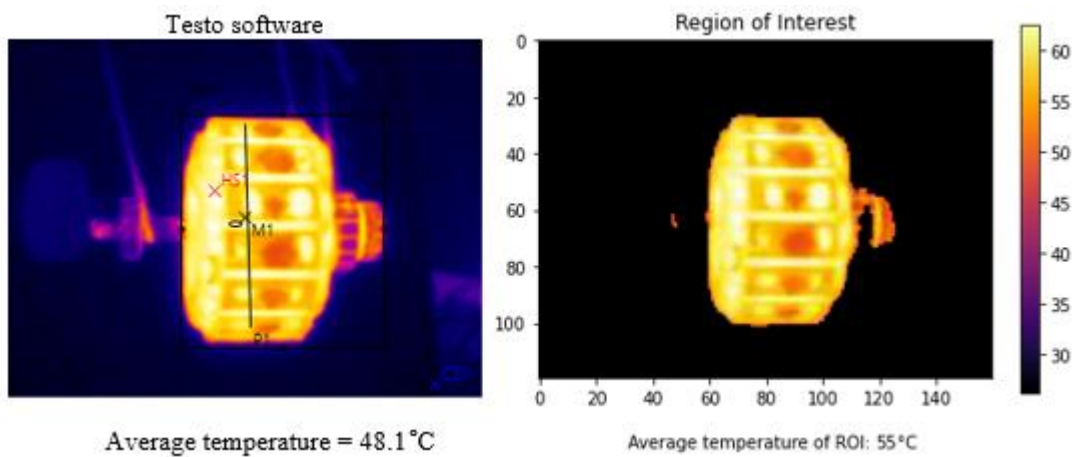


Figure 4-7 Comparison between Testo Software and ROI which is Testo have average temperature of 48.1 °C meanwhile ROI 55 °C

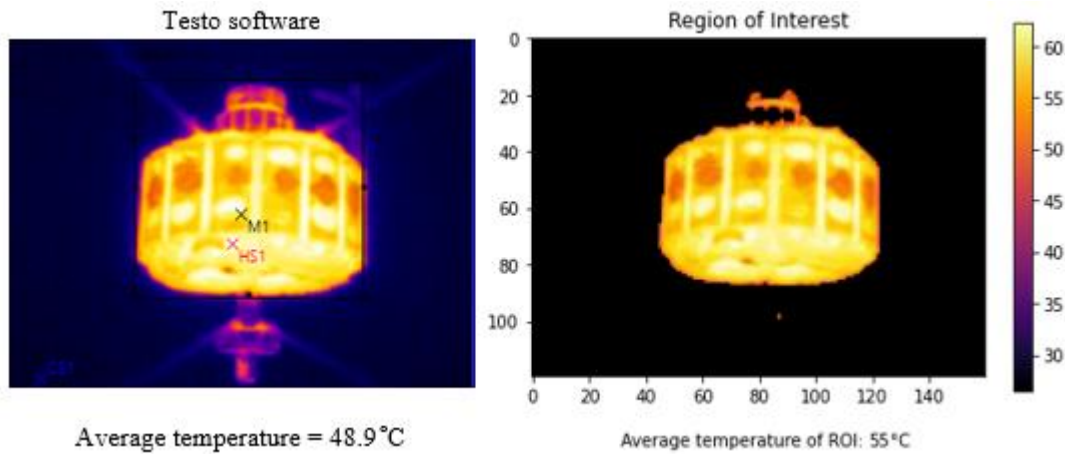


Figure 4-8 Comparison between Testo Software and ROI which is Testo have average temperature of 48.9 °C meanwhile ROI 55 °C

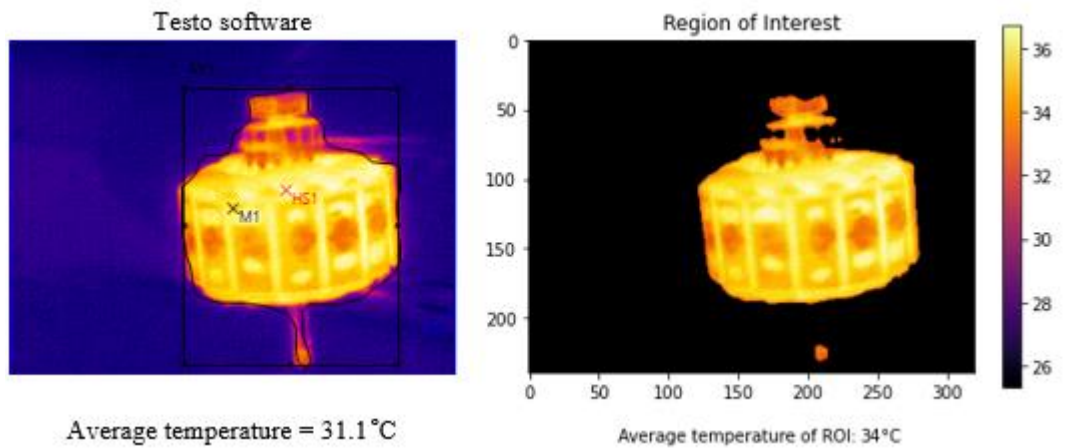


Figure 4-9 Comparison between Testo Software and ROI which is Testo have average temperature of 31.1 °C meanwhile ROI 34 °C

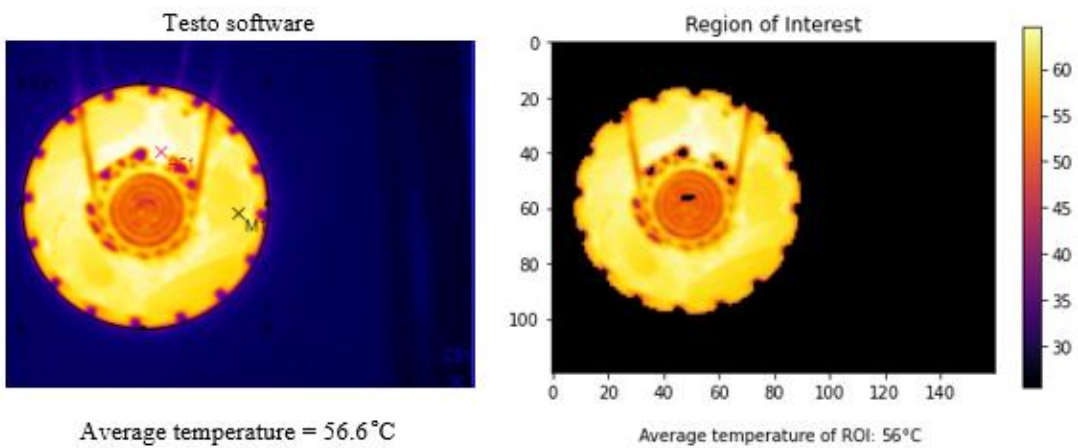


Figure 4-10 Comparison between Testo Software and ROI which is Testo have average temperature of 56.6 °C meanwhile ROI 56 °C

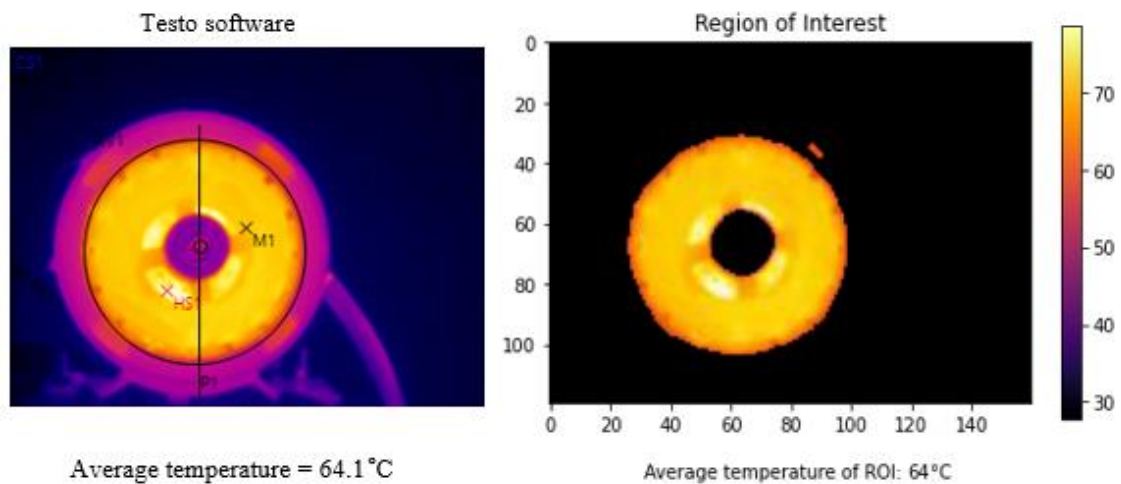


Figure 4-11 Comparison between Testo Software and ROI which is Testo have average temperature of 64.1 °C meanwhile ROI 64 °C

For Figure 4-1, the output is a little bit different. This is due to the Testo's ROI which include the low temperature hotspot in the ROI section thus making the output value differ. This same scenario can also be observed at Figure 4-5, Figure 4-6, and Figure 4-11.

Referring to Figure 4-2, 4-3, 4-4, 4-7, 4-8, 4-9, 4-10, the thresholding method able to fully eliminate the low temperature area of the image. By achieving this, the ROI average temperature is more accurate because the undesired area is completely eliminated.

The result is achieved by utilizing the intensity for each individual pixels in the image. This is because grayscale image contain an intensity value which vary from 0 (black) to 255 (white), so by thresholding the intensity value, the ROI can be achieved. Thresholding procedure used to determine an intensity value called as threshold and threshold separate the desired classed [25].

The software's ROI is not very accurate. This is because the region needs to be set manually with the given tools which are rectangle, circle, ellipse, polygon and whole image. Due to this, during ROI process some of the background image is also in the ROI

area. These shapes have limits when they do not fit with the shape of the area to be defined, either by excluding or including irrelevant data in the thermal image analysis. As a result, inaccuracy may be added into the analysis of certain thermal images.

4.3 Analysis

Table 4-1 Comparing the result between Testo and Thresholding Method

No.	Testo IRSoft Software	ROI using Thresholding Method	Difference between Testo's Software and Thresholding method%
1.	64.3 °C	63 °C	2.0 %
2.	41.5 °C	43 °C	3.5 %
3.	47.6 °C	53 °C	10.2 %
4.	38.3 °C	39 °C	1.8%
5.	54.4 °C	57 °C	4.6%
6.	55.2 °C	58 °C	4.8%
7.	41.8 °C	55 °C	24%
8.	48.9 °C	55 °C	11%
9.	31.1 °C	34°C	8.5%
10.	56.6 °C	56 °C	1.1%
11.	64.1 °C	64°C	0.2%

Table 4-1 above shows the first row have 2% lower average temperature reading from Testo, which is 64.3 °C meanwhile tenth is 1.1% and eleventh is 0.2% have lower average temperature reading. Due to high threshold value, the ROI will be smaller thus resulting lower average temperature reading. From second row until ninth row, the ROI for thresholding method giving out higher output compared to Testo's software. For further reference can be viewed Figure 4-2 until Figure 4-9, as shown in the figure the Testo's software have a very large ROI area compared to thresholding method. Large ROI area also resulting the background image will be inside the ROI area.

CHAPTER 5

CONCLUSION

5.1 Conclusion

The thermal image software (Testo) has certain limitations, mainly because it was designed for general use and did not allow for the identification of a ROI with a custom shape. The drawbacks of existing software were overcome by creating a system that allows users to upload the thermal image, regardless of a specific shape. This project successfully eliminates the issue of irrelevant region that affecting the value of ROI.

5.2 Future Recommendation

To strengthen this project in the future, some suggestions have been noted there is still work that has to be done for ROI and average temperature to make it more accurate. The suggestion is, we may measure the DC motor by using thermocouple or hardware to compare the result. By doing this, ROI will be more accurate since it has a real data to be compared to. Other improvement is, using other algorithm for segmentation method which can improve its accuracy.

REFERENCES

- [1] V. Pašagić and M. Mužević, "Infrared Thermography in," vol. 59, pp. 123–130, 2008.
- [2] X. F. Z. L. R. Zhang, "An Infrared Thermal Imaging Approach with Cooling Pre-treatment for Monitoring Cracks inside Metal Plate," pp. 2992–2997, 2020.
- [3] N. N. Chen, B. Li, Y. Fan, and M. S. Lin, "A segmentation algorithm for thermal paint image," *Proc. 2006 Int. Conf. Mach. Learn. Cybern.*, vol. 2006, no. August, pp. 3842–3846, 2006, doi: 10.1109/ICMLC.2006.258695.
- [4] S. Bagavathiappan, B. B. Lahiri, T. Saravanan, J. Philip, and T. Jayakumar, "Infrared thermography for condition monitoring - A review," *Infrared Phys. Technol.*, vol. 60, pp. 35–55, 2013, doi: 10.1016/j.infrared.2013.03.006.
- [5] A. K. Al-Musawi, F. Anayi, and M. Packianather, "Three-phase induction motor fault detection based on thermal image segmentation," *Infrared Phys. Technol.*, vol. 104, no. November 2019, p. 103140, 2020, doi: 10.1016/j.infrared.2019.103140.
- [6] P. Karvelis *et al.*, "An automated thermographic image segmentation method for induction motor fault diagnosis," *IECON Proc. (Industrial Electron. Conf.)*, pp. 3396–3402, 2014, doi: 10.1109/IECON.2014.7049001.
- [7] P. Guruprasad, "Overview Of Different Thresholding Methods In Image Processing," *TEQIP Spons. 3rd Natl. Conf. ETACC*, no. June, 2020.
- [8] M. S. Jadin and S. Taib, "Infrared image enhancement and segmentation for extracting the thermal anomalies in electrical equipment," *Elektron. ir Elektrotehnika*, vol. 4, no. 4, pp. 107–112, 2012, doi: 10.5755/j01.eee.120.4.1465.
- [9] M. A. Ansari and R. S. Anand, "Region based segmentation and image analysis with application to medical imaging," *IET Semin. Dig.*, vol. 2007, no. 2, pp. 724–729, 2007, doi: 10.1049/ic:20070707.
- [10] Er. Nirpjeet Kaur and Er. Rajpreet Kaur, "A review on various methods of image thresholding," *Int. J. Comput. Sci. Eng.*, vol. 3, no. 10, p. 3441, 2011, [Online]. Available: <http://citeseerx.ist.psu.edu/viewdoc/download;jsessionid=32ED7C9749BB7EEA8CF5F FC3AD55B70A?doi=10.1.1.302.8307&rep=rep1&type=pdf>.
- [11] S. N and V. S, "Image Segmentation By Using Thresholding Techniques For Medical Images," *Comput. Sci. Eng. An Int. J.*, vol. 6, no. 1, pp. 1–13, 2016, doi: 10.5121/cseij.2016.6101.

- [12] S. Zhou, P. Yang, and W. Xie, "Infrared image segmentation based on Otsu and genetic algorithm," *2011 Int. Conf. Multimed. Technol. ICMT 2011*, pp. 5421–5424, 2011, doi: 10.1109/ICMT.2011.6003109.
- [13] H. G. Kaganami and Z. Beiji, "Region-based segmentation versus edge detection," *IIH-MSP 2009 - 2009 5th Int. Conf. Intell. Inf. Hiding Multimed. Signal Process.*, pp. 1217–1221, 2009, doi: 10.1109/IIH-MSP.2009.13.
- [14] B. Sankur, "Survey over image thresholding techniques and quantitative performance evaluation," *J. Electron. Imaging*, vol. 13, no. 1, p. 146, 2004, doi: 10.1117/1.1631315.
- [15] J. Dickens and J. Green, "Segmentation techniques for extracting humans from thermal images," *4th Robot. Mechatronics Conf. South Africa*, no. November 2011, 2011, [Online]. Available: <http://researchspace.csir.co.za/dspace/handle/10204/5553>.
- [16] A. K. Chaubey, "Comparison of The Local and Global Thresholding Methods in Image Segmentation," *World J. Res. Rev.*, vol. 2, no. 1, pp. 1–4, 2016.
- [17] A. Krishnaveni, R. Shankar, and S. Duraisamy, "A review on various image thresholding methods for mammogram image segmentation," *Compliance Eng. J.*, vol. 11, no. 2, pp. 414–426, 2020, [Online]. Available: <http://ijceng.com/gallery/46-cej-2727.f.pdf>.
- [18] M. A. Rahman, M. F. I. Amin, and M. Hamada, "Edge detection technique by histogram processing with canny edge detector," *Proc. 3rd IEEE Int. Conf. Knowl. Innov. Invent. 2020, ICKII 2020*, pp. 128–131, 2020, doi: 10.1109/ICKII50300.2020.9318922.
- [19] P. P. Acharjya, R. Das, and D. Ghoshal, "Study and Comparison of Different Edge Detectors for Image Segmentation," *Glob. J. Comput. Sci. Technol. Graph. Vis.*, vol. 12, no. 13, pp. 29–32, 2012.
- [20] G. N. Chaple, R. D. Daruwala, and M. S. Gofane, "Comparisons of Robert, Prewitt, Sobel operator based edge detection methods for real time uses on FPGA," *Proc. - Int. Conf. Technol. Sustain. Dev. ICTSD 2015*, no. 1, pp. 4–7, 2015, doi: 10.1109/ICTSD.2015.7095920.
- [21] R. Maini and H. Aggarwal, "Study and comparison of various image edge detection techniques," *Int. J. Image Process.*, vol. 3, no. 1, pp. 1–11, 2009.
- [22] Ş. Öztürk and B. Akdemir, "Comparison of Edge Detection Algorithms for Texture Analysis on Glass Production," *Procedia - Soc. Behav. Sci.*, vol. 195, pp. 2675–2682, 2015, doi: 10.1016/j.sbspro.2015.06.477.
- [23] Y. Song and H. Yan, "Image Segmentation Techniques Overview," *AMS 2017 - Asia Model. Symp. 2017 11th Int. Conf. Math. Model. Comput. Simul.*, pp. 103–107, 2018,

doi: 10.1109/AMS.2017.24.

- [24] S. Singh and R. Singh, "Comparison of various edge detection techniques," *2015 Int. Conf. Comput. Sustain. Glob. Dev. INDIACom 2015*, pp. 393–396, 2015, doi: 10.14257/ijcip.2016.9.2.13.
- [25] H. P. Narkhede, "Review of Image Segmentation Techniques," *Int. J. Sci. Mod. Eng.*, no. 18, pp. 2319–6386, 2013.
- [26] X. Font-Aragones, M. Faundez-Zanuy, and J. Mekyska, "Thermal hand image segmentation for biometric recognition," *IEEE Aerosp. Electron. Syst. Mag.*, vol. 28, no. 6, pp. 4–14, 2013, doi: 10.1109/MAES.2013.6533739.
- [27] M. Suguna, S. Mohamed Mansoor Roomi, and I. Sanofer, "Fault localisation of electrical equipments using thermal imaging technique," *Proc. IEEE Int. Conf. Emerg. Technol. Trends Comput. Commun. Electr. Eng. ICETT 2016*, pp. 1–3, 2017, doi: 10.1109/ICETT.2016.7873778.
- [28] T. H. Yoon, K. S. Kim, J. W. Lee, D. J. Kim, and C. G. Song, "Image segmentation of human forearms in infrared image," *Annu. Int. Conf. IEEE Eng. Med. Biol. - Proc.*, pp. 2762–2765, 2006, doi: 10.1109/IEMBS.2006.260706.
- [29] Y. Y. Chen, W. S. Chen, and H. S. Ni, "Image segmentation in thermal images," *Proc. IEEE Int. Conf. Ind. Technol.*, vol. 2016-May, pp. 1507–1512, 2016, doi: 10.1109/ICIT.2016.7474983.
- [30] A. Duarte *et al.*, "Segmentation Algorithms for Thermal Images," *Procedia Technol.*, vol. 16, pp. 1560–1569, 2014, doi: 10.1016/j.protcy.2014.10.178.
- [31] N. F. Abdullah, A. A. Wahab, and M. A. H. Rasid, "Study of temperature rise in small brushed DC motor components under different speed," *IOP Conf. Ser. Mater. Sci. Eng.*, vol. 469, no. 1, pp. 1–6, 2019, doi: 10.1088/1757-899X/469/1/012098.

APPENDIX A

```
import cv2 as cv
import numpy as np
import pandas as pd
from google.colab.patches import cv2_imshow
import skimage.io
import skimage.color
import skimage.filters
import matplotlib.pyplot as plt

#-----LOAD EXCEL-----#
data = pd.read_excel(r'/content/SR000272.xlsx')
df = pd.DataFrame(data)

max = df.max().max()
print('\nMaximum Temperature\n-----')
print(max)

min = df.min().min()
print('\nMinimum Minimum\n-----')
print(min)

#-----LOAD IMAGE-----#
img = skimage.io.imread("/content/SR000272.BMT")
fig, ax = plt.subplots()
plt.imshow(img)
gray_image = skimage.color.rgb2gray(img)

#blur the image to reduce noise
blurred_image = skimage.filters.gaussian(gray_image, sigma=1.0)
fig, ax = plt.subplots()
plt.imshow(blurred_image, cmap='gray')

#histogram of the blur image
histogram, bin_edges = np.histogram(blurred_image, bins=256,
range=(0.0, 1.0))
fig, ax = plt.subplots()
plt.plot(bin_edges[0:-1], histogram)
plt.title("Grayscale Histogram")
plt.xlabel("grayscale value")
plt.ylabel("pixels")
plt.xlim(0, 1.0)
plt.show()

t= 0.4
binary_mask = blurred_image > t
thresh=binary_mask
```

```

fig, ax = plt.subplots()
plt.imshow(binary_mask, cmap='gray')
plt.show()

images = cv.imread("/content/SR000272.BMT", 0)
t_int = t/0.0039215686274

#THRESH BINARY,to count number of pixel of ROI
ret,thresh = cv.threshold(images,t_int,255,cv.THRESH_BINARY)
pixels = cv.countNonZero(thresh) #use cv.countNonZero to
calculate total pixels by ignoring 0 value

#THRESH TO ZERO, to count intensity
ret,thresh1=cv.threshold(images,t_int,255,cv.THRESH_TOZERO)

#calculation
a=np.array([thresh])
b=np.sum(a)
a1=np.array([thresh1])
b1=np.sum(a1)
pixels1 = cv.countNonZero(thresh1)

#DISPLAY OUTPUT
selection = img.copy()
selection[~binary_mask] = 0

fig, ax = plt.subplots()

#AVERAGE TEMPERATURE#
range = (df.max().max())-(df.min().min())
print("range =", range)
temp_ratio = range/255
print("ratio =", temp_ratio)

#Colorbar
eqn=round(((b1)/(pixels1))*temp_ratio)+min)
plt.imshow(selection, cmap = 'inferno',vmin=min,
vmax=max),plt.title("Region of Interest")
plt.colorbar()
plt.figtext(0.58, 0.01,"Average temperature of ROI:",
ha="right", fontsize=10)
plt.figtext(0.6, 0.01,eqn, ha="center", fontsize=10)
plt.figtext(0.63, 0.01,"°C", ha="center", fontsize=10)

```